

EXAMINATION OF WATER PHASE TRANSITIONS IN BLACK SPRUCE BY MAGNETIC RESONANCE AND MAGNETIC RESONANCE IMAGING

Clevan Lamason

PhD Candidate
Faculty of Forestry and Environmental Management
E-mail: clamason@unb.ca

Bryce MacMillan

Research Scientist
E-mail: bryce@unb.ca

*Bruce Balcom**

Professor and Director
Magnetic Resonance Imaging Center
Department of Physics
E-mail: bjb@unb.ca

Brigitte Leblon

Professor
Faculty of Forestry and Environmental Management
University of New Brunswick, NB, Canada
E-mail: bleblon@unb.ca

Zarin Pirouz

Senior Research Scientist
FPInnovations
Vancouver, BC, Canada
E-mail: zarin.pirouz@fpinnovations.ca

(Received October 2013)

Abstract. This study examines the phase transitions of water in wood by magnetic resonance and magnetic resonance imaging. The goal was to observe and understand the behavior of water below 0°C in wood. The species studied, black spruce (*Picea mariana* Mill.), presented one abrupt phase change that occurred at about -3°C, which was attributed to the phase transition of free water. A more diffuse change occurred below -60°C, which was attributed to a phase transition of bound water. A recently developed portable unilateral magnetic resonance instrument is demonstrated as a powerful tool in the study of water in wood. This portable magnet used a bulk spin-spin relaxation time measurement that quantifies observable bound and free water in wood. Imaging was used to verify the unilateral magnetic resonance results and to better understand realistic freeze-thaw behavior of log samples in the field. A ring boundary behavior during the thawing process was observed, and likewise there were differences in the thawing behaviors of heartwood and sapwood samples.

Keywords: Water phase transition, bound water, free water, freeze-thaw, magnetic resonance, magnetic resonance imaging, portable unilateral magnetic resonance, SPRITE.

* Corresponding author

INTRODUCTION

Wood is a hygroscopic and anisotropic material whose properties are deeply influenced by the presence of water. Measurements of wood moisture content are therefore of considerable importance. Water in wood can exist as either absorbed water (free water) in the cell lumens and intercellular spaces or as adsorbed water (bound water) within the cell walls (Siau 1971; Panshin and de Zeeuw 1980; Walker 2006). The FSP is defined as the moisture content at which all the absorbed water has been removed but the cell walls are still fully saturated. This occurs at about 30% MC for most species (Skaar 1988; Walker 2006). The FSP is a critical parameter because most properties of wood are altered by changes in moisture content below the FSP. A number of physical and mechanical properties of wood are independent of moisture content at higher moisture contents, but these properties are found to change at lower moisture contents as the bound water is removed (Siau 1971; FPL 2010). For example, wood shrinks as bound water is removed.

Numerous magnetic resonance (MR) and magnetic resonance imaging (MRI) studies on wood have been reported in the literature. Conventional MR and MRI techniques were used to study wood anatomy and structure (Hall et al 1986; Wang and Chang 1986; Filbotte et al 1990), wood decay (Filbotte et al 1990), and wood preservation (Meder et al 1999). MR and MRI techniques have been used to estimate moisture content in wood pellets (Nyström and Dahlquist 2004) and in drying lumber (Hall et al 1986; Menon et al 1987; Quick et al 1990; Araujo et al 1992; Hameury and Sterley 2006; Almeida et al 2007; Stenstrom et al 2009). Most MRI studies consider relatively wet wood because conventional MRI techniques are not quantitative at low moisture contents. There are no previous MR or MRI studies of freeze-thaw behavior in wood.

There are relatively few studies of freeze-thaw behavior in wood using other techniques. van Dyk and Rice (2005) investigated the use of ultrasonic wave velocity as a measure of moisture

content in frozen wood samples. They found a strong inverse relationship between ultrasonic wave velocity and moisture content for both frozen and unfrozen lumber. Sparks et al (2000) used time-domain reflectometry to measure the water content of frozen plant material. They found that more than 25% of the water in wood was not frozen even at temperatures of -15°C . They attributed this to water in the cell wall, which is potentially transportable at temperatures below 0°C . Karenlampi et al (2005) and Zelinka et al (2012) used differential scanning calorimetry (DSC) to examine phase transitions of wood cell wall water. Karenlampi et al (2005) found that sample preparation was important for DSC measurements of water interacting with cellulose and cell wall components. Freezing behavior was dependent on sample preparation.

From the literature, it is known that free water in the lumen will freeze at slightly below 0°C (Walker 2006). Berthold et al (1996) and Olsson and Salmén (2004) have proposed a solution model in which cell wall water uptake occurs at specific sites by cluster adsorption. The adsorbed water, both the nonfreezing bound water (equivalent to monomolecular adsorption [Brunauer, Emmett and Teller {BET} theory]) and the freezing bound water (equivalent to polymolecular adsorption [BET theory]) clustered around the polar groups and their cations. They reported that the freezing bound water did not form normal ice structures because of the influence of the polar groups of the cell wall materials, and this water had nonbulk water-like thermodynamic parameters.

The purpose of this study was to further investigate the behavior of water in wood at low temperatures with MR and MRI. In particular, we were interested in the phase transitions of water in black spruce (*Picea mariana* Mill.). These were investigated with standard bulk MR, with MRI, and with unilateral MR, a new instrumental approach with increased flexibility and portability. It was our aim to demonstrate that MR and MRI are well suited to quantify water content of frozen and thawed black spruce wood samples and thereby to observe phase changes

in temperature-dependent measurements. In this study, we assumed that MR and MRI signal intensities were not affected by any changes in FSP and other chemical effects on wood at low temperatures. Likewise, changes in FSP at freezing conditions were assumed to be very minimal. Similar studies have been undertaken in other porous materials, notably the MRI study by Prado et al (1998) on freeze-thaw behaviors of concrete.

MR is a physical phenomenon in which nuclei with a magnetic moment are excited by radio-frequency (RF) magnetic fields and then detected by induction in the RF probe. The MR phenomenon occurs at a specific frequency, the resonance frequency, which depends on the strength of the magnetic field and on the magnetic properties of the nuclei under study. According to the Larmor equation, the resonance frequency is directly dependent on both the strength of the magnetic field and the gyromagnetic ratio (Liang and Lauterbur 2000).

$$\omega = \gamma B_0 \quad (1)$$

where ω is the resonance frequency also known as the Larmor frequency (MHz). The gyromagnetic ratio (γ) is a constant dependent on the nuclei under study; 42.58 MHz/Tesla for 1H . B_0 is the static magnetic field strength (Tesla).

In MR, the term relaxation describes specific processes by which nuclear magnetization in nonequilibrium states returns to equilibrium. Two different time constants characterize the longitudinal (spin-lattice) and transverse (spin-spin) relaxations. T_1 (spin-lattice relaxation time) is a measure of the time required for a spin system to return to thermal equilibrium with its surroundings (lattice). T_1 governs the recovery of the longitudinal magnetization. T_2 (spin-spin relaxation time) governs the decay of transverse magnetization caused by spin-spin interactions. T_2^* accounts for the effect of both T_2 decay and magnetic field inhomogeneities (Liang and Lauterbur 2000). The MR signal typically decays exponentially with T_2 and T_2^* , which are related to the type of water (bound and free) in wood.

For porous media such as wood, in which water is present in void spaces or trapped in micropores, the spin-spin relaxation rate ($\frac{1}{T_2}$) is expressed as the weighted sum of the surface relaxation rate and the bulk relaxation rate (Wong 1999). In the case of rapid exchange of water between the two environments, there is an average relaxation rate.

$$\frac{1}{T_2} = \frac{n}{T_{2S}} + \frac{m}{T_{2B}}, n + m = 1 \quad (2)$$

where $\frac{1}{T_{2S}}$ is the surface relaxation rate, and $\frac{1}{T_{2B}}$ is the bulk relaxation rate. The variables n and m are the relative quantities of water in the surface and bulk environments.

In the case of water in wood, there are three different water environments: (1) water in the cell walls is motionally restricted and conventionally considered bound water. Stamm (1964) used the sigmoidal adsorption curve proposed by Brunauer, Emmett, and Teller (1938), the BET equation, to calculate the average number of molecular layers of water at fiber saturation. Stamm reported 6.5 layers for sitka spruce (*Picea sitchensis*) and 7.5 layers for sugar maple (*Acer saccharum*). The moisture content needed to form a monomolecular surface layer within the amorphous regions of cellulose is about 5% (Stamm 1964; Walker 2006). The BET theory considered the cell wall water as a surface phenomenon with a strongly adsorbed monolayer and less strongly bound polymeric water.

There are two different types of lumen water. One is the bulk lumen water (2), which is considerably more mobile, and the other is a small fraction that adheres to the lumen walls (3). The observed relaxation rate from the water in the lumen (conventionally called free water) is the weighted average rate of the surface water and bulk water, as given in Eq 2 (Wong 1999). Typically, there is more bulk water than surface water when the wood is green, but the surface relaxation rate is much greater than the bulk relaxation rate. The bulk and surface water in the lumen together are considered free water.

Two bulk measurements of MR signal intensity and MR signal lifetime, namely the free induction decay (FID) and the Carr Purcell Meiboom Gill (CPMG), were used in this study. The FID is the most basic MR measurement. It is a one pulse measure of MR signal intensity and of lifetime T_2^* . It was used here with a superconducting magnet. The CPMG measurement is a spin echo pulse sequence consisting of a 90° RF pulse followed by an echo train induced by successive 180° RF pulses. It allows measurements of the spin-spin relaxation time, T_2 . It was used here with both a superconducting magnet and a unilateral magnet.

The FID and CPMG measurements are not spatially resolved. By contrast, MRI requires spatially encoding the MR signal using magnetic field gradients, allowing the spatial distribution of a sample's MR signal to be reconstructed in an image format. The single point ramped imaging with T_1 enhancement (SPRITE) MRI measurement (Balcom et al 1996) was used in this study. A detailed description of SPRITE has been published in Balcom et al (1996). Here, we summarize a few relevant features.

SPRITE is a pure phase-encoded MRI measurement that does not require echo formation. It uses ramped magnetic field gradients and brief-duration broadband RF pulses, which permit rapid image acquisition in cases where the signal lifetimes are short, as in the case of low water content wood materials (MacMillan et al 2002, 2011).

For a centric scan SPRITE image using an RF excitation pulse with uniform RF flip angle (α), the signal intensity denoted by S , at any point in the image, is determined by Eq 3 (Halse et al 2003):

$$S = S_0 e^{-t_p/T_2^*} \sin \alpha \quad (3)$$

where S_0 is the signal intensity at $t = 0$. S_0 is proportional to the amount of observable water. t_p is the phase encode time, and T_2^* is the effective transverse signal lifetime. T_2^* is a function of both the intrinsic transverse relaxation time, T_2 ,

and the local magnetic field inhomogeneity, ΔB_0 , as shown in Eq 4:

$$\frac{1}{T_2^*} = \frac{1}{T_2} + \gamma \Delta B_0 \quad (4)$$

where γ is the nuclear gyromagnetic ratio. Generally, for water in wood, $t_p \ll T_2^*$ meaning that the *SPRITE* signal intensity did not suffer from T_2^* attenuation and signal intensity was directly proportional to liquid water content. T_2^* was long for liquids but short for solids. Therefore, when water freezes, the signal intensity decreases dramatically (according to Eq 3), because $t_p \gg T_2^*$. Frozen water (ice) will not be visible in the image (Prado et al 1998).

The *SPRITE* MRI measurement was used with the superconducting magnet instrument to resolve 3D space within the sample, whereas the unilateral magnet integrates the signal from a finite volume within the sample. The superconducting magnet instrument is a more mature technology than the unilateral magnet. *SPRITE* MRI measurements were compared with the CPMG measurements using the unilateral magnet.

MATERIALS AND METHODS

Thawing and freezing measurements of the MR signal were undertaken on black spruce. For thawing studies, three black spruce sapwood samples and one black spruce heartwood sample of approximately $25 \times 75 \times 75$ mm were prepared from an initially frozen green wood disk. The top portion of the sapwood sample contained the bark. The green wood disk was wrapped with cellophane and kept in the freezer until the time of measurement to prevent moisture loss. The sapwood samples had bark on the outer part of the sample. One of the sapwood samples and the heartwood sample were used for imaging measurements, whereas the remaining two sapwood samples were used for unilateral magnet measurements. The samples were initially frozen at approximately -20°C and then allowed to thaw, during the measurements, at ambient temperature.

For thawing studies, bulk MR and MRI measurements were undertaken. The 3D *SPRITE* MRI images were acquired using a Nalorac (Nalorac Cryogenics Inc., Martinez, CA) 2.4-Tesla horizontal bore superconducting magnet instrument. The ambient temperature surrounding the sample was 12°C. *SPRITE* 3D imaging parameters were number of scans = 4, time between gradient steps = 2 ms, time between conical gradient trajectories = 300 ms, encoding time = 112 μ s, maximum gradient = 6 G/cm, field of view (FOV) = 120 mm, RF pulse width = 10.0 μ s, RF flip angle = 8°, and total acquisition time = 10 min.

The unilateral permanent magnet, designed and fabricated in the University of New Brunswick Magnetic Resonance Imaging Center, is a lightweight three-magnet array (Marble et al 2007), which offers open access and portability. Figure 1 shows the unilateral magnet along with the RF coil. Figure 2 shows the magnetic field along the central vertical line above the surface of the unilateral magnet used in this study. The unilateral magnet has a homogenous magnetic field of 10 mm³ volume located approximately 13 mm away from the top of the magnet.

For the unilateral magnet measurements, the ambient temperature was 3°C. This was achieved

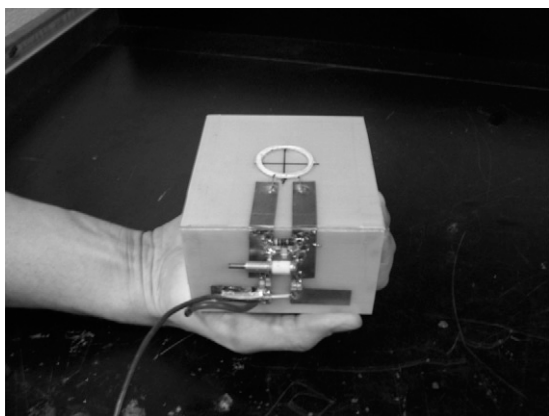


Figure 1. The unilateral magnet device used in this study. The white circle on the face of the magnet array is the radio-frequency probe. The sensor is connected to the *Bruker Minispec* console, and the radiofrequency probe is placed adjacent to the wood sample for moisture content measurements.

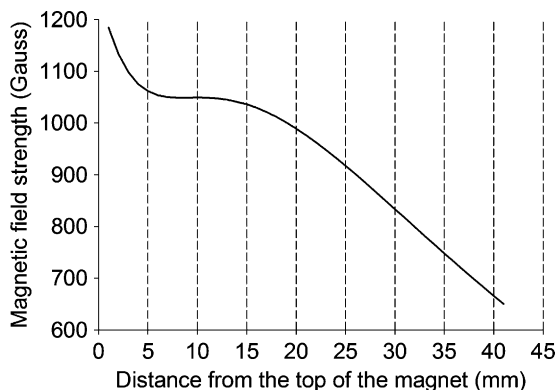


Figure 2. Magnetic field along the central vertical line of the magnet array. The center of the homogeneous spot is 13 mm from the surface of the magnet. This permits measurement of signal within a finite volume inside the sample and not just on the surface. In the case of wood logs, measurements of magnetic resonance signal in the sapwood are therefore possible without first removing the bark.

by placing the unilateral magnet and the sample inside an insulated and actively cooled box to slow the thawing process. Measurements were taken continuously until the sample thawed completely. Each sample was wrapped in cellophane, and no significant mass loss was observed during the measurements. The CPMG measurement, undertaken on a 4.46-MHz resonance frequency unilateral magnet instrument, was used to measure the spin–spin relaxation time (T_2). CPMG measurement parameters were 90° pulse length = 10 μ s, scans = 512, number of echoes = 128, and acquisition time was about 5 min.

For freezing studies, we used 2D spiral *SPRITE* MRI measurements on a 3 × 25 × 25-mm sapwood sample with no visual defects. The sample was prepared from the same green wood disk as for the thawing study. The dimensions of the small sapwood sample allowed it to fit a sample holder for temperature control. The small sapwood sample permitted rapid and more uniform temperature changes compared with the original sample (25 × 75 × 75 mm) in the 3D *SPRITE* measurements. The sample was wrapped in cellophane to prevent mass loss during the course of the measurements. It was left at ambient temperature for approximately 1 h before commencement of the measurements. Sample mass

was measured before and after measurements, and no significant mass loss was observed. For temperature control, the sample was positioned in a heated-cooled air stream inside a glass transfer line specially designed to fit the geometrical specifications of the imaging system. The air temperature was controlled with an Omega (Omega Engineering, Stamford, CT) CN6072A-P2 temperature controller using a platinum resistance temperature device (RTD) in close proximity to the sample. The air temperature was stable to within $\pm 0.3^\circ\text{C}$. MRI was undertaken at temperatures that ranged from -1 to -100°C .

Two-dimensional Spiral *SPRITE* MRI (Szomolanyi et al 2001) measurements were performed during freezing. The *SPRITE* experimental parameters included number of scans = 32, time between gradient steps = 2 ms, time between spirals = 500 ms, encoding time = 72 μs , maximum gradient = 24.5 G/cm, FOV = 38 mm, RF pulse width = 1.0 μs , RF flip angle = 8° , and total acquisition time = 3.2 min.

RESULTS AND DISCUSSION

Thawing of Black Spruce Sapwood

Free induction decay and single point ramped imaging with T_1 enhancement MRI measurements with a superconducting magnet.

The gravimetric moisture content of the sapwood sample used was 111%. Figure 3 shows the time-domain FID acquired for the black spruce sapwood sample as it thawed from 0.15 to 6.20 h. The sample temperature during the thawing process changed from -20 to 10°C . Two changes occurred in the bulk FID measurement. First, T_2^* increased from 330 μs to 1.2 ms as a new liquid water population emerged as the sample thawed. Second, the signal intensity increased by a factor of 3.1 as thawing proceeded. The signal grew as the population of liquid water increased as a result of the thawing process. The relative change of the signal intensity was found to be proportional to the ratio of bound and free water in these green black spruce sapwood samples. The thawing measurements suggested that we are observing a phase change

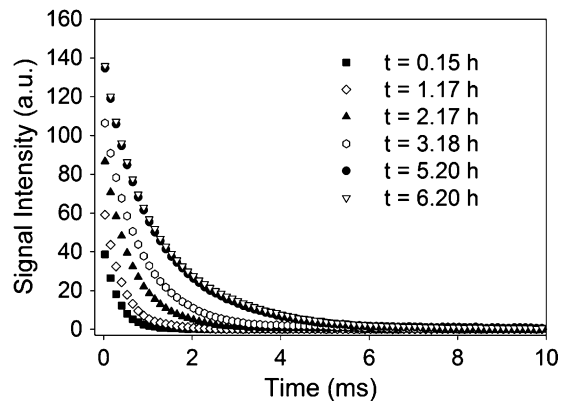


Figure 3. Time-domain bulk free induction decay (FID) signal as the black spruce sapwood sample thawed from 0.15 to 6.20 h using the Nalorac 2.4-Tesla horizontal bore superconducting magnet. The time between points on the FID was 5 μs . No short lifetime signal component was observed. The T_2^* increased from 330 μs to 1.2 ms. The signal amplitude increased by a factor of 3.1 as the sample temperature increased from -20 to 10°C .

of the free water. The bound water was unfrozen and is observable throughout the thawing process. This is consistent with the conceptual definition of FSP. At 111% MC, the amount of free water is approximately three times the amount of bound water assuming a FSP of about 30% MC.

Figure 4 shows 2D slices from the 3D MRI data sets in the transverse and tangential planes as a function of time at ambient temperature while the sapwood sample (approximately $25 \times 75 \times 75$ mm) thawed. Similar to the bulk FID results, signal increased as a function of thawing time. In these images, the frozen water, with its characteristically short T_2^* , was not observed. Regions of high signal intensity (white) are regions with high concentration of liquid water. There was slight curvature and the presence of bark on the top of the transverse plane. The rate of thawing front progression on the transverse plane was different for each side because of the presence of bark and heartwood. The sapwood sample contained a portion of the neighboring heartwood region, and this was evident in the thawing pattern of the sample image.

A moving ring boundary of thawing was observed in the images as the sapwood sample

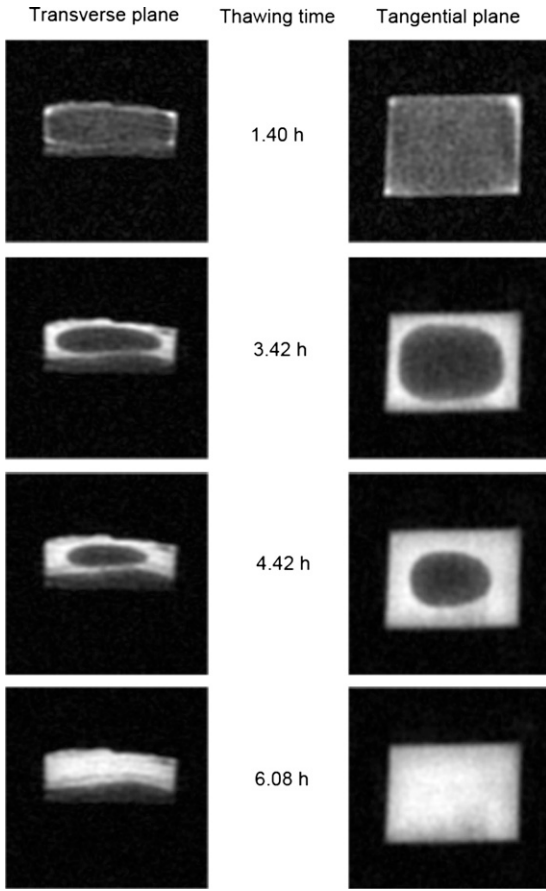


Figure 4. Single-point ramped imaging with T_1 enhancement (SPRITE) magnetic resonance imaging of a black spruce sapwood sample in the transverse (left) and tangential (right) planes as a function of thawing time at ambient temperature. A moving ring boundary of thawing front was observed.

thawed (Fig 4). Figure 5 shows the displacement of the boundary as a function of the square root of thawing time in two orthogonal directions, parallel to the grain and across the grain. Carslaw and Jaeger (1959) showed that for a one-dimensional sample, under ideal conditions, the progression of a thawing front would be proportional to the square root of the product of time and thermal conductivity of the melted phase. This is not the case with our data (Fig 5) probably because of the 3D nature of the phenomenon. Thawing occurs because of heat transport in all three directions at the same time in our measurement.

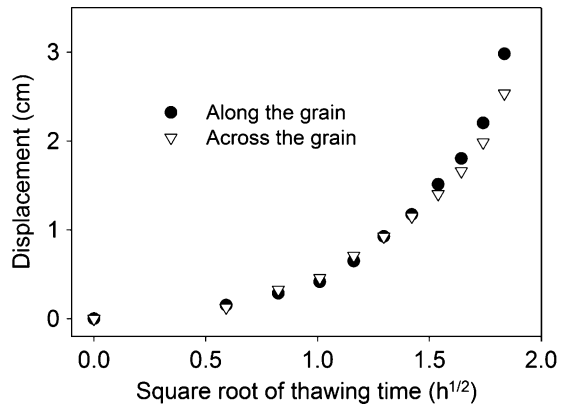


Figure 5. Displacement of the ring boundary of the thawing front both along and across the grain directions from Fig 4 as a function of the square root of thawing time. Displacement increased nonlinearly as the black spruce sapwood sample thawed. The thawing front progression was nearly identical both along and across the grain.

Using the relationship developed by Carslaw and Jaeger (1959), we estimated that the early time rate of thawing front progression was 12 mm/h. This prediction was based on literature values of the relevant thermodynamic properties. However, Fig 5 shows that the measured early time rate of thawing front progression was approximately 70% of the theoretical prediction. The theoretical prediction did not include the thermal properties of the substrate, ie wood. Given the assumptions involved in the theoretical prediction (thermal conductivities such as conductivity, thermal diffusivity, and specific heat and latent heat of fusion approximated by water and ice with a one-dimensional model), the agreement was remarkably good.

Although the thermal conductivity of wet wood is reported to be different for wood material along the grain and across the grain (Steinhagen 1977; Panshin and de Zeeuw 1980; FPL 2010), no significant differences in the thawing front progression occurred as a function of grain orientation (Fig 5). Literature values for thermal conductivity of wood vary significantly with the species in question, with density, and with moisture content (Steinhagen 1977; Panshin and de Zeeuw 1980; FPL 2010). The theoretical prediction that thawing front progression depends

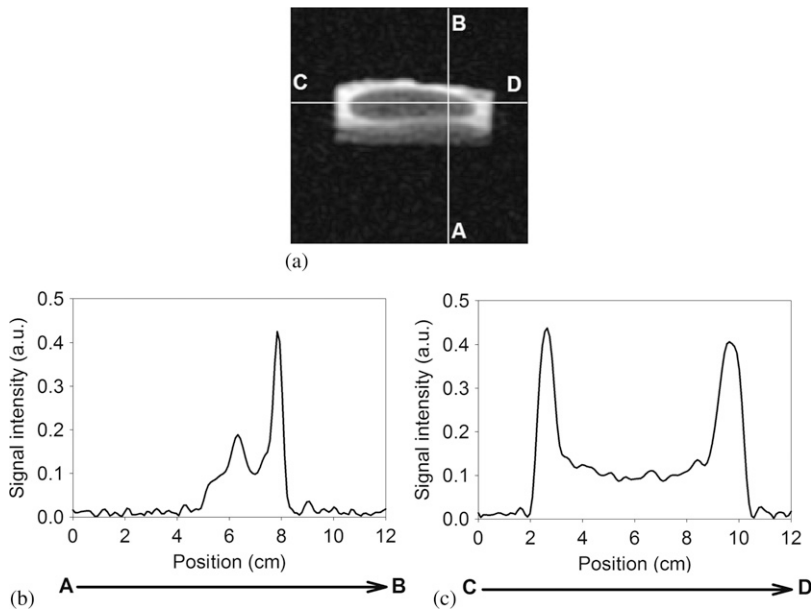


Figure 6. One-dimensional profiles (b–c) extracted from the transverse image in Fig 4 at the positions indicated by the white lines (a). The signal intensity in the frozen sapwood region is similar to that in the unfrozen heartwood (bottom region of the image [a]).

on the square root of thermal conductivity means we do not anticipate great sensitivity to grain direction given that thermal conductivities vary by only a factor of two (Panshin and de Zeeuw 1980; FPL 2010).

The signal intensity from the heartwood was equal to the signal in the still frozen region of the sapwood (Fig 6). The signal from the frozen sapwood came from the bound water, which is known to be unfrozen at these temperatures (Merchant 1957; Tarkow 1971; Sparks et al 2000; Karenlampi et al 2005; Zelinka et al 2012). This suggests that the water in this particular heartwood was mostly bound water because the moisture content of the sample was 31.1%. At this moisture content, by the conceptual definition of FSP, most of the water is in the cell wall. The water in the heartwood sample was also not frozen at these temperatures, and the only phase transitions occurring were in the free water component of the sapwood. This is in agreement with Merchant (1957) and Tarkow (1971). Merchant (1957) concluded that the cell wall water is not frozen at -20°C . Tarkow

(1971) concluded that at least some adsorbed water does not change mobility until very low temperatures ($<-80^{\circ}\text{C}$).

Carr Purcell Meiboom Gill measurements using a unilateral magnet. The gravimetric moisture content of the sapwood sample used for the unilateral magnet measurements was 109%. A two-component T_2 fit was used to analyze the CPMG T_2 decay data (Fig 7). The total signal increased as the sample thawed. The liquid water population increased accordingly. Signal magnitude was proportional to the amount of unfrozen water in the sample. The short and long lifetime components corresponded to the bound and free water, respectively. These results are in agreement with Riggin et al (1979) and Araujo et al (1992), who reported relaxation times of water in wood that corresponded to cell wall water and lumen water. The moisture content was derived from the y-intercepts of Fig 7 with the help of a calibrated standard.

Figure 7 shows time-domain CPMG decay plots of signal intensity as sapwood samples thawed

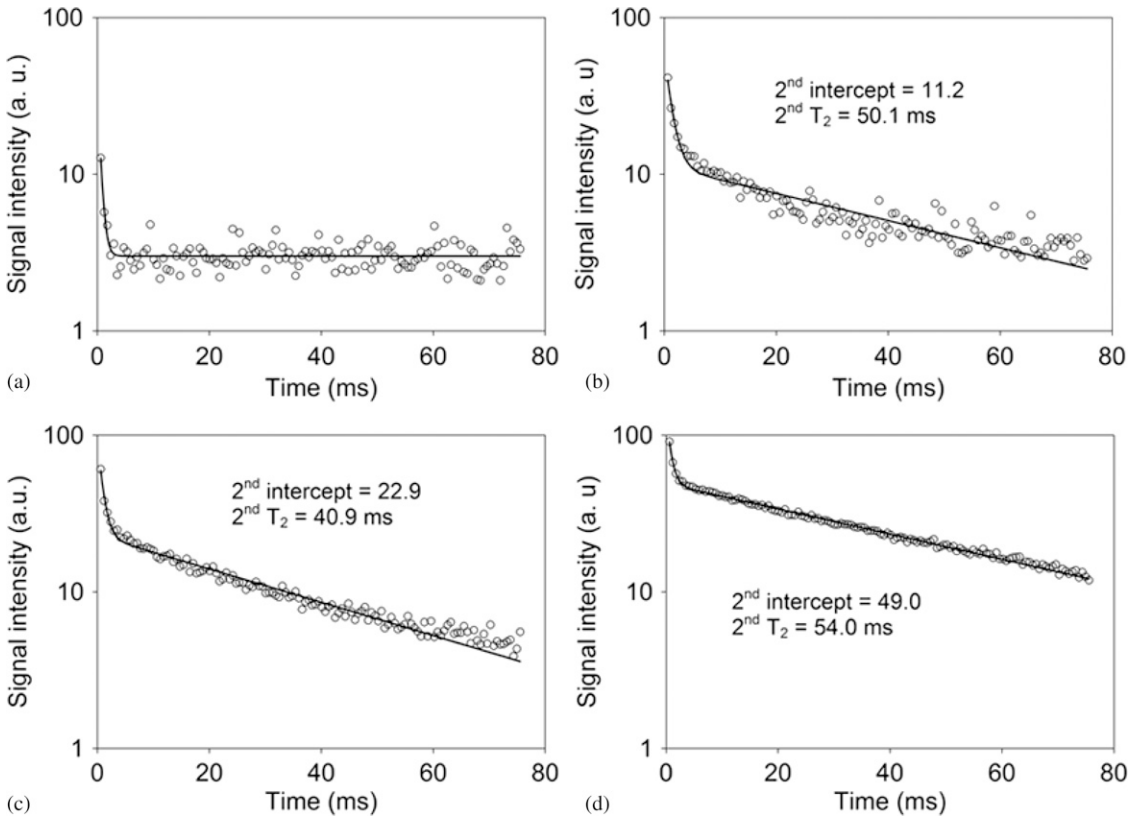


Figure 7. Biexponential Carr Purcell Meiboom Gill (CPMG) decay plots of signal intensity of samples thawed to various extents. A unilateral magnet with CPMG measurements was used. The initial sample temperature was -20°C and the surrounding temperature was 3°C . At thawing time of (a) 6 min, no phase transition of water occurred; (b) 295 min, phase transition of the long lifetime signal component (free water) was observed; (c) 345 min; and (d) 405 min. The amount of free water increased as more liquid water was created from sample thawing.

to various extents. The time constant of the short lifetime component is too short to measure accurately given the dead time of the RF probe used ($\approx 120 \mu\text{s}$). However, based on the data points observed, the short T_2 component is estimated to be 0.5-0.9 ms. The long T_2 components varied between 40.9 and 54.0 ms. Only the long lifetime components were further analyzed.

Figure 8 shows the signal intensities of the long signal lifetime component (free water) acquired by CPMG measurement as the sample thawed. The total signal increased as the black spruce sapwood sample thawed. The signal intensity is proportional to the amount of unfrozen water in the sample. Most of the water in the sample is still frozen until 200 min. The unilateral magnet

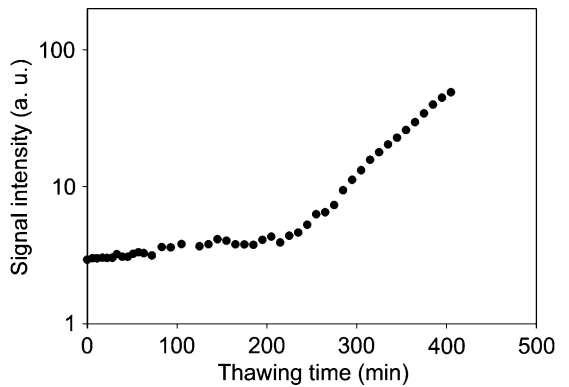


Figure 8. Semilog plot of the signal intensity of the long lifetime components (free water) of Fig 7 as a function of thawing time of black spruce sapwood. The ring boundary of thawing emerges in the sensitive volume commencing at 200 min.

used for these measurements has a region of homogenous magnetic field of 10-mm³ volume that is located approximately 13 mm away from the top of the magnet. This permits excitation and detection of signal inside this restricted volume. In Fig 8, the signal intensity increased after 200 min of thawing. The increase in signal intensity indicates the start of thawing as the ring boundary of thawing moved through the sensitive spot. The signal continued to increase after 200 min as the water in the sample melted and the amount of unfrozen water increased.

Thawing of Black Spruce Heartwood

The gravimetric moisture content of the heartwood sample was 31.1%. FID and *SPRITE* measurements, similar to those undertaken with sapwood samples, were performed on the heartwood sample. Virtually no changes occurred in either the FID data (Fig 9) or the 2D images (Fig 10), even after 4.6 h of thawing. Because the heartwood sample used in these measurements was estimated to be at the FSP, most of the water was located in the cell walls (bound water). This supports the assertion that water in the heartwood (mostly bound water at FSP) is unfrozen at -20°C . The T_2^* was constant at approximately 400 μs . This T_2^* value was very similar to the T_2^* estimation from the FID mea-

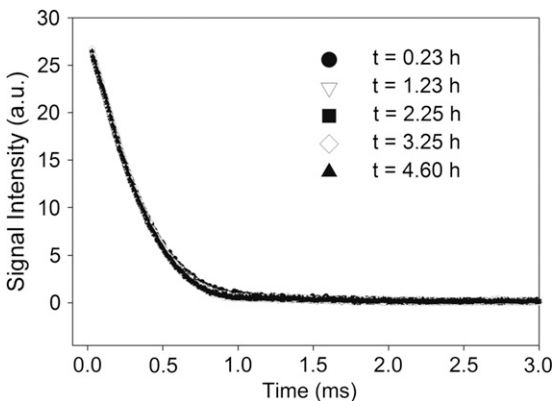


Figure 9. Time-domain bulk free induction decay (FID) signal as the black spruce heartwood sample thawed from 0.23 to 4.60 h using the Nalorac 2.4-Tesla horizontal bore superconducting magnet. The T_2^* signal lifetime was constant at 400 μs . No water phase transition was observed.

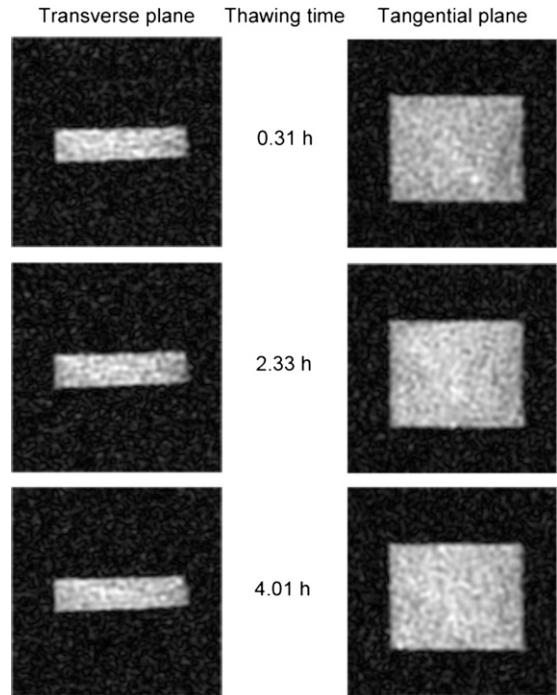


Figure 10. Single-point ramped imaging with T_1 enhancement (*SPRITE*) magnetic resonance imaging of a black spruce heartwood sample in the transverse (left) and tangential (right) planes as a function of thawing time. No changes occurred even after 4.6 h of warming. The heartwood sample was at the FSP. Therefore, most of the water was in the cell walls. Bound water was not frozen at measurement conditions.

surements of frozen black spruce sapwood, which was 330 μs . We conclude that the frozen heartwood signal came from bound water. If the moisture content of heartwood is above FSP, which is normally the case for this species, we would anticipate some free water populations to be frozen at the initial temperature, which was -20°C .

Freezing of Black Spruce Sample

Sapwood was used for the freezing study to permit observation of both bound and free water. We did not use a heartwood sample in these measurements because the heartwood sample was estimated to be at FSP. The gravimetric moisture content of the sapwood sample used was 110%. Figure 11 shows the bulk FID as a

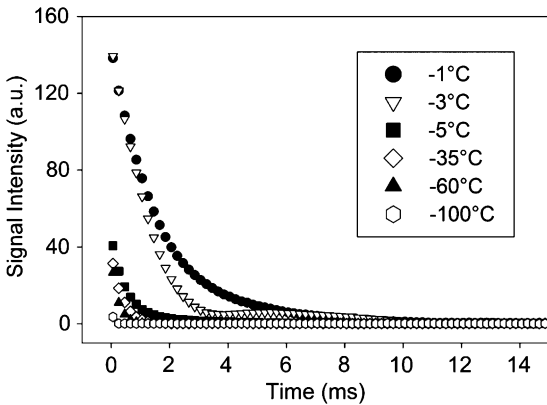


Figure 11. Time-domain bulk free induction decay (FID) as a function of time for different temperatures as the black spruce sapwood sample froze. Signal decreased with temperature as water underwent a phase change. The time between points on the FID was 5 μ s.

function of time for different temperatures as the black spruce sapwood sample froze. The bulk FID signal decreased as the temperature decreased from -1 to -100°C . Signal from frozen water was undetectable with our MR apparatus.

Figures 12 and 13 show bulk signal intensity vs temperature as the black spruce sapwood sample froze. The water in the sapwood sample underwent two phase transitions. The plots were

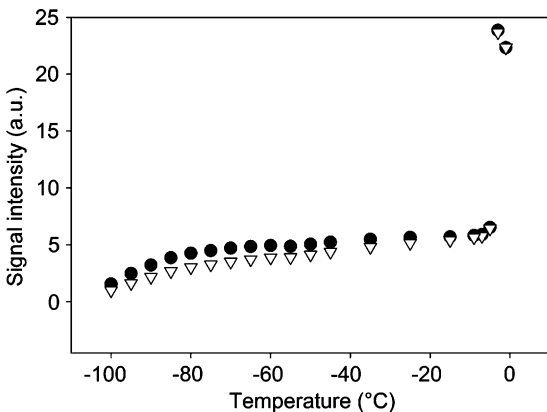


Figure 12. Bulk magnetic resonance signal intensity vs temperature as the black spruce sapwood sample froze: original data (●) and corrected for temperature (▽) as defined by Curie's Law. Carr Purcell Meiboom Gill measurement was undertaken. An abrupt phase change of free water occurred at -3°C . A second phase change (bound water) was observed below -60°C .

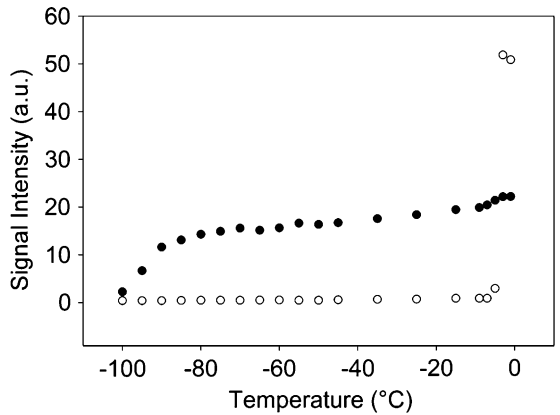


Figure 13. Bulk signal intensity of bound (●) and free (○) water vs temperature from the corrected data of Fig 12 as the black spruce sapwood sample froze. Carr Purcell Meiboom Gill measurement was undertaken. The ratio of signal from free and bound water was approximately 3:1.

corrected for the effect of temperature on the sample magnetization. As the sample temperature decreased, the sample magnetization increased as explained by Curie's Law (Kittel 1976). Curie's law states that the sample magnetization is inversely proportional to the sample temperature in Kelvin. This temperature effect is minimal at the beginning of the freezing experiment, but the effect can be up to 37% at the later stages of the freezing experiment. Results show that one abrupt phase change occurred at -3°C (Fig 12). A less abrupt phase change occurred below -60°C (Fig 12).

Figure 13 indicates that the first change is attributed to the transition of free water to ice. We believe that the phase change at lower temperatures was caused by a phase transition of the bound water. Bound water can exist in either a strongly bound monolayer or less strongly bound multilayer. Other researchers refer to the monomolecular adsorption as the nonfreezing bound water and the polymolecular adsorption as the freezing bound water. The bound water underwent a phase change but did not form normal ice structures because of the influence of the polar groups of the cell wall material, and this water had nonbulk water-like thermodynamic properties. Unlike free water in the lumen, the phase transition of bound water was depressed

to substantially below 0°C (Berthold et al 1996; Olsson and Salméén 2004; Walker 2006).

The signal intensity before the first phase transition (at which free water freezes) was three times higher than the signal intensity after the first phase transition. This is consistent with the ratio of bound and free water in this sample, which was 3:1 using the FID measurements (Fig 3).

Figures 13 and 14 show the signal intensities and T_2 values of free and bound water as a function of temperature from the data in Fig 12. Signal intensity and T_2 were determined using CPMG measurements. Figures 13 and 14 suggest that the abrupt transition in free water occurred at -3°C . Signal from free water was no longer observable below this temperature. The T_2 of bound water was much shorter than the T_2 of free water (Riggin et al 1979; Araujo et al 1992). There was a slight decrease of T_2 from bound water as temperature decreased. The phase transition of bound water occurred across a wider temperature range than the abrupt transition of the free water. Movement of bound water is restricted because it is confined in the cell wall through hydrogen bonds.

Figure 15 shows 2D images of a black spruce sapwood sample as it froze. The images clearly

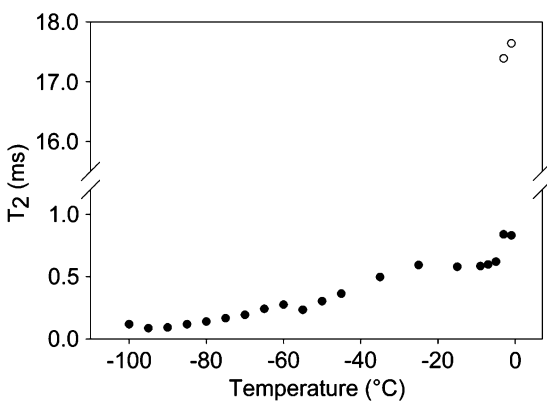


Figure 14. Bulk T_2 of bound (●) and free (○) water vs temperature from the corrected data of Fig 12 as the black spruce sapwood sample froze. Carr Purcell Meiboom Gill measurement was undertaken. The T_2 of bound water was much shorter than the T_2 of free water.

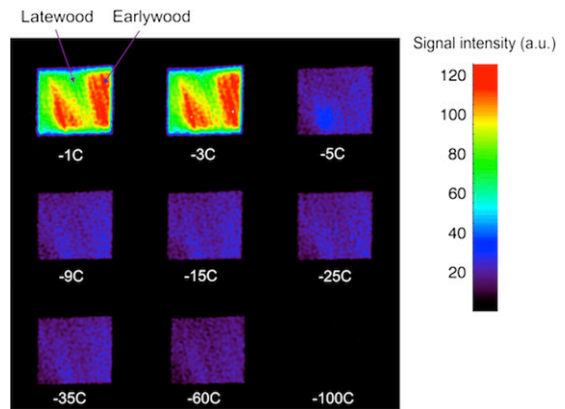


Figure 15. Two-dimensional spiral single point ramped imaging with T_1 enhancement (SPRITE) images of a black spruce sapwood sample ($2 \times 25 \times 25$ mm). Each image is 64×64 pixels. High signal intensity corresponds to high concentration of liquid water. Phase transition of free water occurred at -3°C . A nonzero signal from -5 to -60°C suggests that bound water was not frozen at these temperatures. Prior to the freezing phase transition of free water, the signal of earlywood was twice the signal of latewood in a growth ring.

show an abrupt signal intensity change that occurred between -3 and -5°C . Even at -60°C , the signal was nonzero, which means that bound water in this sample was still not frozen. The 2D images at both -1 and -3°C also show distinct differences between earlywood and latewood. The signal of the earlywood was twice as high as that of the latewood. The difference in signal was associated with the larger size of the lumen of the earlywood tracheids (Panshin and de Zeeuw 1980), which allows the earlywood to accommodate more free water. This result is consistent with the findings of other studies of moisture content in earlywood and latewood of green coniferous species. The moisture content in the early sapwood is much greater than in latewood. The coniferous species studied include *Pinus radiata* D. Don. (Harris 1961; Kininmonth and Whitehouse 1991) and *Pseudotsuga menziesii* Franco (Harris 1961; Raczkowski et al 2000).

The SPRITE MRI measurements determined the phase transition of bound water, which is challenging for other techniques, such as calorimetry-based methods.

CONCLUSIONS

The use of a unilateral MR instrument and the SPRITE MRI measurement in a series of thawing and freezing experiments established the possibility of studying water phase transitions in frozen wood samples. An abrupt phase transition of free water was observed at -3°C . A more diffuse phase transition occurred below -60°C . This was attributed to a phase change of bound water.

The unilateral MR instrument and SPRITE MRI measurement used allowed measurements of relative quantities of bound and free water in wood. None of the MR and MRI measurements undertaken were able to measure frozen water directly. We may infer the amount of frozen water by temperature-dependent measurements of samples that were initially unfrozen. However, direct MR and MRI measurements of frozen samples do not permit an estimation of the amount of frozen water. This is true for small laboratory samples and log samples in the field.

Also, the results demonstrate that unilateral MR is a powerful tool to monitor water quantity and quantify bound and free water in green log samples. Another advantage is that it is portable. The unilateral magnet used in this study is currently being evaluated in measuring moisture content of drying logs with a through-bark measurement.

REFERENCES

- Almeida G, Gagne S, Hernandez RE (2007) A NMR study of water distribution in hardwoods at several equilibrium moisture contents. *Wood Sci Technol* 41(4):293-307.
- Araujo CD, Mackay AL, Hailey JRT, Whittall KP, Le H (1992) Proton magnetic resonance techniques for characterization of water in wood: Application to white spruce. *Wood Sci Technol* 26(2):101-113.
- Balcom BJ, MacGregor RP, Beyea SD, Green DP, Armstrong RL, Bremner TW (1996) Single point ramped imaging with T_1 enhancement (SPRITE). *J Magn Reson A* 123(1):131-134.
- Berthold J, Rinaudo M, Salmén L (1996) Association of water to polar groups; Estimations by an adsorption model for lingo-cellulosic materials. *Colloid Surface A* 112:117-129.
- Brunauer S, Emmett PH, Teller EJ (1938) Adsorption of gases in multilayers. *J Am Chem Soc* 60:309-319.
- Carslaw HS, Jaeger JC (1959) Conduction of heat in solids. 2nd ed. Oxford University Press, New York, NY. 510 pp.
- Filbotte S, Menon RS, MacKay AL, Hailey JRT (1990) Proton magnetic resonance of western red cedar. *Wood Fiber Sci* 22(4):362-376.
- FPL (2010) Wood handbook: Wood as an engineering material. Gen Tech Rep FPL-GTR-190. USDA For Serv Forest Prod Lab, Madison, WI. 508 pp.
- Hall LD, Rajanayagam V, Stewart WA, Steiner PR (1986) Magnetic resonance imaging of wood. *Can J For Res* 16(2):423-426.
- Halse M, Goodyear DJ, MacMillan B, Szomolanyi P, Matheson D, Balcom BJ (2003) Centric scan SPRITE magnetic resonance imaging. *J Magn Reson* 165(2):219-229.
- Hameury S, Sterley M (2006) Magnetic resonance imaging of moisture distribution in *Pinus sylvestris* L. exposed to daily indoor relative humidity fluctuations. *Wood Mater Sci Eng* 1:116-126.
- Harris JM (1961) Water conduction in the stems of certain conifers. *Nature* 189(4765):678-679.
- Karenlampi PP, Tynjala P, Strom P (2005) Phase transformations of wood cell wall water. *J Wood Sci* 51(2):118-123.
- Kininmonth JA, Whitehouse LJ (1991) Properties and uses of New Zealand radiata pine. Vol. 1. Wood properties. New Zealand Forest Research Institute, Jan Bryce Printers Ltd., Rotorua. Pages 74-76.
- Kittel C (1976) Introduction to solid state physics. 5th ed. John Wiley & sons, Inc., New York, NY. Page 440.
- Liang Z-P, Lauterbur PC (2000) Principle of magnetic resonance imaging—A signal processing perspective. The Institute of Electrical and Electronics Engineers, Inc., New York, NY. Pages 57-76.
- MacMillan B, Schneider MH, Sharp AR, Balcom BJ (2002) Magnetic resonance imaging of water concentration in low moisture content wood. *Wood Fiber Sci* 34(2):276-286.
- MacMillan B, Veliyulin E, Lamason C, Balcom BJ (2011) Quantitative magnetic resonance measurements of low moisture content wood. *Can J For Res* 41:2158-2162.
- Marble AE, Mastikhin IV, Colpitts BG, Balcom BJ (2007) A compact permanent magnet array with a remote homogenous field. *J Magn Reson* 186(1):100-104.
- Meder R, Franich RA, Callaghan PT (1999) 11B magnetic resonance imaging and MAS spectroscopy of trimethylborate-treated radiata pine wood. *Solid State Nucl Mag* 15(1):69-72.
- Menon RS, MacKay AL, Hailey JRT, Bloom M, Burgess AE, Swanson JS (1987) An NMR determination of the physiological water distribution in wood during drying. *J Appl Polym Sci* 23(11):3147-3154.
- Merchant MV (1957) A study of water-swollen cellulose fibres which have been liquid-exchanged and dried from hydrocarbons. *Tappi J* 40(9):771-781.
- Nyström J, Dahlquist E (2004) Methods for determination of moisture content in woodchips for power plants—A review. *Fuel* 83(7-8):773-779.

- Olsson AM, Salmén L (2004) The association of water to cellulose and hemicellulose in paper examined by FTIR spectroscopy. *Carbohydr Res* 339(4):813-818.
- Panshin AJ, de Zeeuw C (1980) *Textbook of wood technology*. 4th ed. McGraw-Hill Publishing Company, New York, NY. 722 pp.
- Prado PJ, Balcom BJ, Beyea SD, Bremner TW, Armstrong RL, Grattan-Bellew PE (1998) Concrete freeze/thaw as studied by magnetic resonance imaging. *Cement Concr Res* 28(2):261-270.
- Quick JJ, Hailey JRT, MacKay AL (1990) Radial moisture profiles of cedar sapwood during drying: A proton magnetic resonance study. *Wood Fiber Sci* 22(4):404-412.
- Raczkowski J, Olek W, Guzenda R (2000) Moisture evaporation rates from sapwood and heartwood samples of Douglas Fir (*Pseudotsuga menziesii* Franco) green wood. *Holz Roh Werkst* 58:247-252.
- Riggin MT, Sharp AR, Kaiser R (1979) Transverse NMR relaxation of water in wood. *J Appl Polym Sci* 23(11):3147-3154.
- Siau JF (1971) *Flow in wood*. 1st ed. Syracuse University Press, Syracuse, NY. 131 pp.
- Skaar C (1988) *Wood-water relations*. Springer-Verlag, New York, NY. 283 pp.
- Sparks JP, Campbell GS, Black RA (2000) Liquid water content of wood tissue at temperatures below 0°C. *Can J For Res* 30(4):624-630.
- Stamm AJ (1964) *Wood and Cellulose Science*. The Ronald Press Company, New York, NY. 549 pp.
- Steinhagen HP (1977) Thermal conductive properties of wood, green or dry, from -40° to +100°C: A literature review. Gen Tech Rep FPL-9. USDA For Serv Forest Prod Lab, Madison, WI.
- Stenstrom S, Bonazzi C, Foucat L (2009) Magnetic resonance imaging for determination of moisture profiles and drying curves. Pages 91-142 in E Tsotsas and AS Mujumdar, eds. *Modern drying technology*. Vol. 2. Experimental techniques. Wiley-VCH, Weinheim, Germany.
- Szomolanyi P, Goodyear D, Balcom BJ, Matheson D (2001) *SPIRAL-SPRITE*: A rapid single point MRI technique for application to porous media. *Magn Reson Imaging* 19(3-4):423-428.
- Tarkow H (1971) On a reinterpretation of anomalous moisture adsorption isobars below 0°C. *Tappi J* 54(4):593.
- van Dyk H, Rice RW (2005) Ultrasonic wave velocity as a moisture indicator in frozen and unfrozen lumber. *Forest Prod J* 55(6):68-72.
- Walker JCF (2006) *Primary wood processing: Principles and practice*. 2nd ed. Springer, Dordrecht, The Netherlands. 603 pp.
- Wang PC, Chang SJ (1986) Nuclear magnetic resonance imaging of wood. *Wood Fiber Sci* 18(2):308-314.
- Wong P (1999) *Methods in the physics of porous media*. Academic Press, San Diego, CA. Pages 337-385.
- Zelinka SL, Lambrecht MJ, Glass SV, Wiedenhoef AC, Yelle DJ (2012) Examination of water phase transitions in loblolly pine and cell wall components by differential scanning calorimetry. *Thermochim Acta* 533:39-45.